Electronic Supplementary Material (ESI) for ChemComm.

† Electronic Supporting Information

Monitoring Nanoparticle Reactivity in Solution: Interaction of L-lysine and Ru Nanoparticles Probed by Chemical Shift Perturbation parallels regioselective H/D exchange

Luis M. Martínez-Prieto,[a,*] Edwin A. Baquero,[a,b] Grégory Pieters, [c] Juan C. Flores,[d] Ernesto de Jesús,[d] Céline Nayral,[a] Fabien Delpech,[a] Piet W. N. M. van Leeuwen,[a] Guy Lippens[e,*] and Bruno Chaudret[a,*]

a LPCNO, Laboratoire de Physique et Chimie des Nano-Objets, Université de Toulouse, CNRS, INSA, UPS 135 avenue de Rangueil, 31077 Toulouse, France.
E-mails: lmmartin@insa-toulouse.fr chaudret@insa-toulouse.fr

b Departamento de Química, Facultad de Ciencias, Universidad Nacional de Colombia, Sede Bogotá, Carrera 30 No. 45-03, 111321 Bogotá, Colombia

c SCBM, CEA, Université Paris Saclay, F-91191, Gif-sur-Yvette, France.

d Departamento de Química Orgánica y Química Inorgánica Universidad de Alcalá, Campus Universitario 28871 Alcalá de Henares, Madrid, Spain.

e LISBP, Université de Toulouse, CNRS, INRA, INSA, UPS 135 avenue de Rangueil, 31077 Toulouse, France.
E-mail: glippens@insa-toulouse.fr

Table of contents

S1. Experimental Section

General considerations and starting materials

All chemical operations were carried out under an argon atmosphere using standard Schlenk and Fisher-Porter tubes, or glove-box techniques. Solvents were purified before use: THF (Sigma-Aldrich) by distillation under an argon atmosphere and pentane (SDS) by filtration on an adequate column in a MBraun purification system.

Ru(COD)(COT) was purchased from Nanomeps Toulouse, CO from Air liquide, ^{13}CO (^{13}C, 99.14%) from Eurisotop, Sodium deuteroxide solution [NaOD (40 wt. % in D_2O), 99%], L-lysine (98%), L-lysine•HCl (99%) and L-lysine•2HCl (98%) from Sigma-Aldrich. All reagents were used as received from the commercial sources.

Thermal Analyses (TGA). TGA analyses were performed in a TGA/DSC 1 STAR System equipped with an ultra-microbalance UMX5, a gas switch GC200 and sensors DTA and DSC. The samples were analyzed through a two-step oxidation/reduction method. First the sample was heated from 25 °C to 700 °C at 10 °C/min under air (2h). After cooling down, it was heated again from 25 °C to 900 °C at 30 °C/min under a gas mixture Ar/H_2 4% (3h).

Wide-angle X-ray scattering (WAXS). WAXS was performed at CEMES-CNRS. Samples were sealed in 1.0 mm diameter Lindemann glass capillaries. The samples were irradiated with graphite monochromatized molybdenum Kα (0.071069 nm) radiation and the X-ray intensity scattered measurements were performed using a dedicated two-axis diffractometer. Radial distribution functions (RDF) were obtained after Fourier transformation of the reduced intensity functions.

Nuclear Magnetic Resonance (NMR). ^1H spectra were recorded on a Bruker Avance 400 spectrometer. For information about equipment for NMR interaction studies, see section S9.

Solid state NMR (MAS-NMR). Solid-state NMR experiments were recorded at the LCC (Toulouse) on a Bruker Avance 400 spectrometer equipped with 2.5 mm probes. Samples were spun between 16 to 20 kHz at the magic angle using ZrO_2 rotors. ^{13}C MAS experiments were performed with a recycle delay of 20 s. ^{13}C CP/MAS spectra were recorded with a recycle delay of 2 s and a contact time of 4 ms. Hahn-echo scheme were synchronized with the spinning rate.

Transmission Electron Microscopy (TEM) and High resolution TEM (HRTEM). Ru NPs were observed by TEM and HRTEM after deposition of a drop of a solution of the isolated nanoparticles after dispersion in THF on a copper grid. TEM analyses were performed at the UMS-Castaing by using a JEOL JEM 1011 CX-T electron microscope operating at 100 kV with a point resolution of 4.5 Å. The approximation of the particles mean size was made through a manual analysis of enlarged micrographs by measuring a

number of particles on a given grid. HRTEM observations were carried out with a JEOL JEM 2010 electron microscope working at 200 kV with a resolution point of 2.35 Å. FFT treatments have been carried out with Digital Micrograph Version 3.7.4.

Infrared spectroscopy (IR). ATR IR-FT spectra were recorded on a Thermo Scientific Nicolet 6700 spectrometer in the range 4000-600 cm^{-1}.

High-performance liquid chromatography (HPLC): HPLC chromatograms were recorded using a Phenomonex chiral column [3126 (D)-penicillamine (ref 00F-3126-E0); 25 cm × 4.6 mm]. Mobile phase: 2mM $CuSO_4$. Flow rate: 1.0 $ml.min^{-1}$. T^a: 22 °C. detector: UV at 254 nm.

Synthesis of water-soluble imidazolium salts

The imidazolium salts **1**-H and **2**-H were synthesized according to the procedure described in the literature.[1]

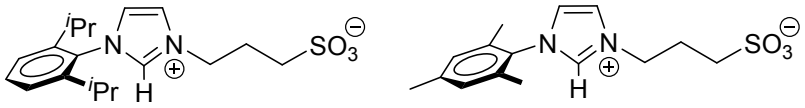

1-H **2-H**

Figure S1. Water-soluble NHC ligands used in this work.

Synthesis of Ru NPs

Ru@PVP was synthesized according to the procedure described in the literature.[2]

Ru@1: A Schlenk flask was charged with **1**-H (56.1 mg, 0.16 mmol, 0.2 equiv.) and KO^tBu (19.7 mg, 0.176 mmol, 0.22 equiv.). The solids were suspended in THF (30 mL) and stirred at r.t. for 20 h. The resulting solution (yellow-orange) was transferred under an argon atmosphere into a 250 mL Fisher-Porter bottle charged with a frozen solution (-80 °C) of Ru(COD)(COT) (250 mg, 0.8 mmol, 1 equiv.) in 80 mL of THF (previously degassed by three freeze-pump cycles). The Fisher-Porter reactor was pressurized with 3 bar of H_2, and the solution was allowed to reach the r.t. whilst the solution was stirred vigorously leading to a black homogeneous solution immediately. The stirring was pursued for

[1] L. R. Moore, S. M. Cooks, M. S. Anderson, H.-J. Schanz, S. T. Griffin, R. D. Rogers, M. C. Kirk, K.H. Shaughnessy *Organometallics* **2006**, *25*, 5151.

[2] (a) Pan, C.; Pelzer, K.; Philippot, K.; Chaudret, B.; Dassenoy, F.; Lecante, P.; Casanove, M. J. *J. Am. Chem. Soc.* **2001**, *123*, 7584 (b) García-Antón, J.; Axet, M. R.; Jansat, S.; Philippot, K.; Chaudret, B.; Pery, T.; Buntkowsky, G.; Limbach, H.-H. *Angew. Chem. Int. Ed.* **2008**, *47*, 2074.

20 h at r.t.. After that, the remaining H_2 pressure was evacuated, the solution was concentrated to 2-3 mL, and 30 mL of pentane were added. The resulting black precipitate was washed twice with pentane (50 mL) and dried overnight under vacuum. The size of the NPs was measured by TEM on a sample of at least 150 nanoparticles, which afforded a mean value of 1.4 (0.2) nm. TGA gave the following Ru content: 58.7 % Ru.

Ru@2: A Schlenk flask was charged with **2**-H (49.1 mg, 0.16 mmol, 0.2 equiv.) and KO^tBu (19.7 mg, 0.176 mmol, 0.22 equiv.). The solids were suspended in THF (30 mL) and stirred at r.t. for 20 h. The resulting solution (yellow-orange) was transferred under argon atmosphere into a 250 mL Fisher-Porter bottle charged with a frozen solution (-80 °C) of Ru(COD)(COT) (250 mg, 0.8 mmol, 1 equiv.) in 80 mL of THF (previously degassed by three freeze-pump cycles). The Fischer-Porter reactor was pressurized with 3 bar of H_2, and the solution was allowed to reach the r.t. whilst the solution was stirred vigorously leading to a black homogeneous solution immediately. The stirring was pursued for 20 h at r.t.. After that, the remaining H_2 pressure was evacuated, the solution was concentrated to 2-3 mL, and 30 mL of pentane were added. The resulting black precipitate was washed twice with pentane (50 mL) and dried overnight under vacuum. The size of the NPs was measured by TEM on a sample of at least 150 nanoparticles, which afforded a mean value of 1.5 (0.3) nm. TGA gave the following Ru content: 61.0 % Ru.

S2. TEM and HRTEM data

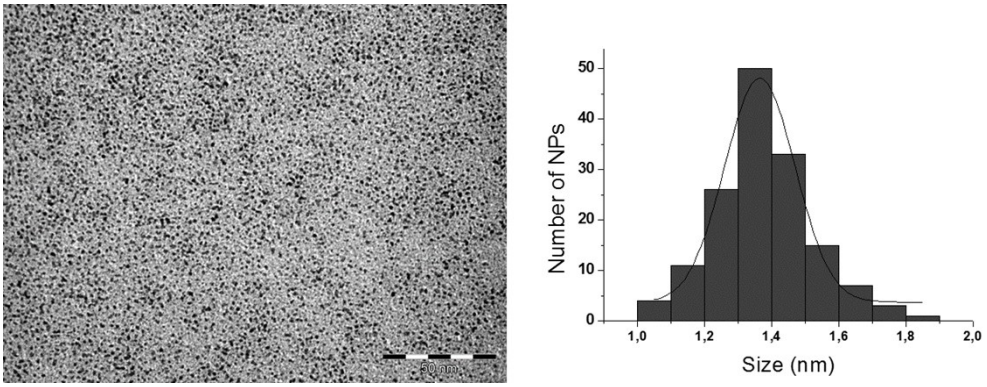

Figure S2. TEM micrograph (left) and the corresponding size histogram (right) of Ru@**1**.

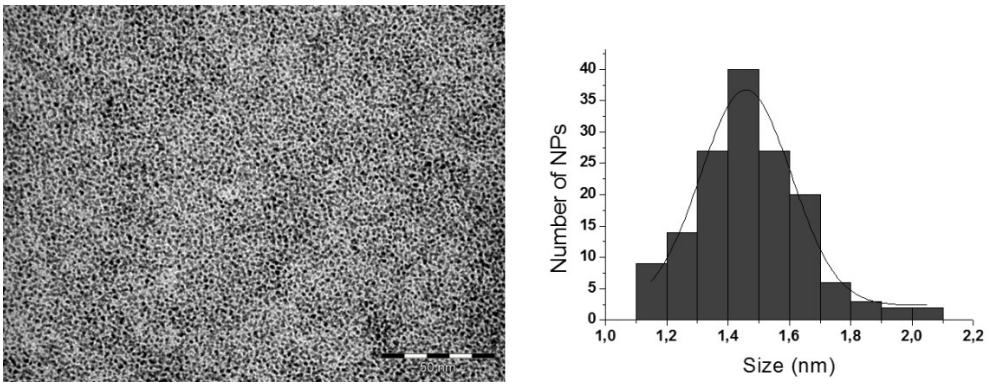

Figure S3. TEM micrograph (left) and the corresponding size histogram (right) of Ru@**2**.

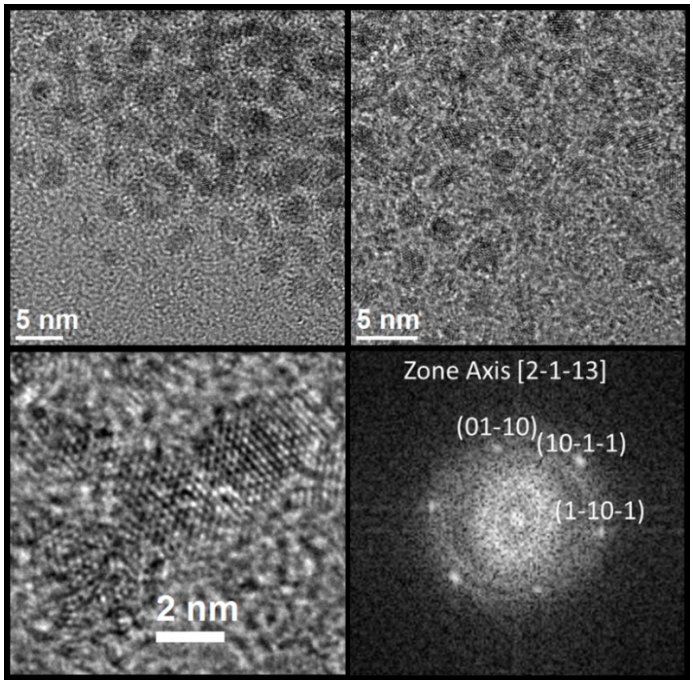

Figure S4. HRTEM micrographs of Ru@**1** (right, top), Ru@**2** (left, top and bottom) and the Fourier Transform Analysis (right, bottom) with planar reflections of Ru@**2**.

S3. WAXS data

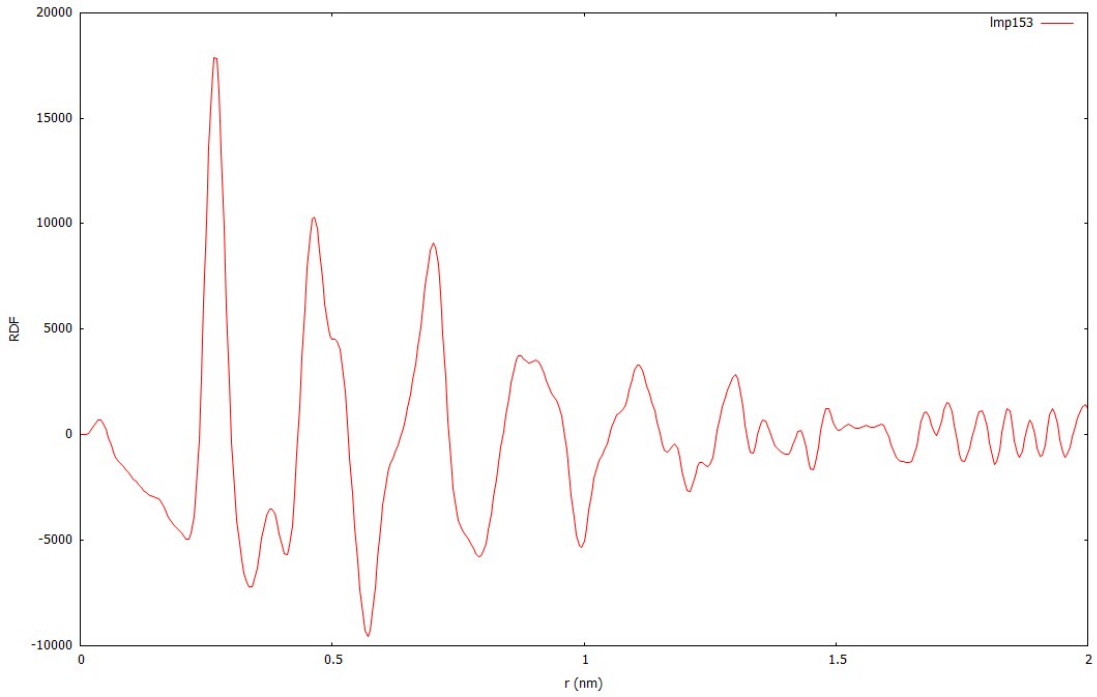

Figure S5. WAXS analysis of Ru@**1**. Metallic Ru particles with a single domain. The pattern is consistent with *hcp* Ru and coherence length is close to 1.5 nm.

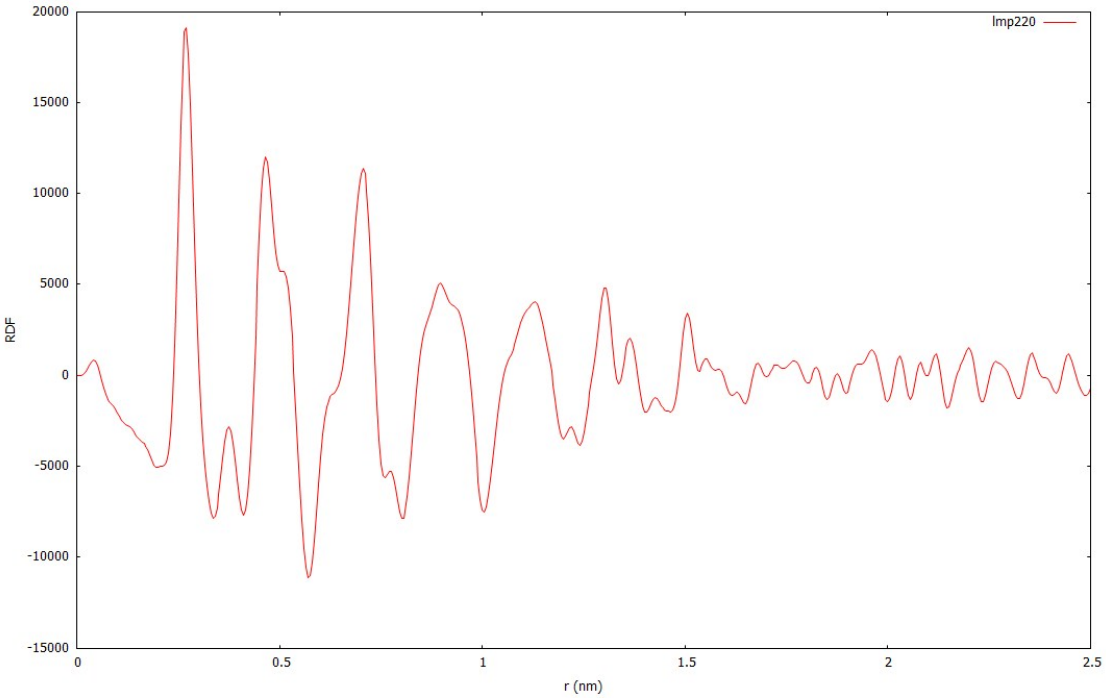

Figure S6. WAXS analysis of Ru@**2**. Metallic Ru particles with a single domain. The pattern is consistent with *hcp* Ru and coherence length is close to 1.5 nm.

S4. FT-IR data

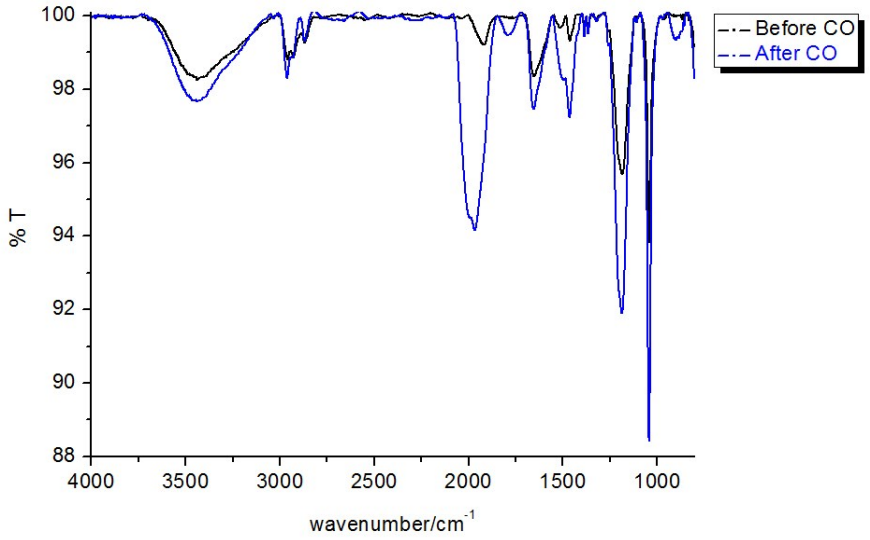

Figure S7. ATR FT-IR spectra of Ru@**1** before (black)* and after (blue) reaction with CO. The spectrum after exposure to CO exhibits the characteristic absorption bands of COb (1771 cm^{-1}) and COt (1962 cm^{-1}).

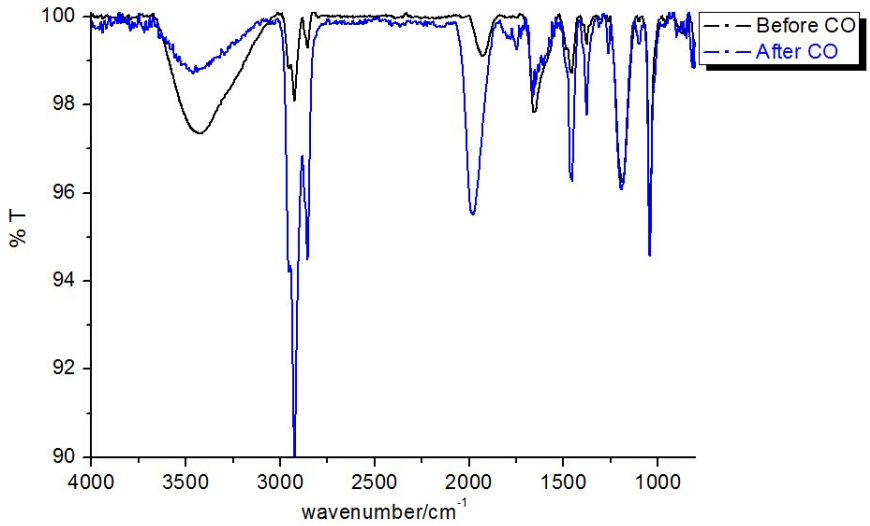

Figure S8. ATR FT-IR spectra of Ru@**2** before (black)* and after (blue) reaction with CO. The spectrum after exposure to CO exhibits the characteristic absorption bands of COb (1767 cm^{-1}) and COt (1978 cm^{-1}).

* FT-IR spectra before (black) exposure to carbon monoxide show a CO absorption band (1916-1922 cm^{-1}) in Figures S7 and S8. This CO was produced during the Ru NPs synthesis through a decarbonylation process of the THF used as solvent[3]

[3] L. M. Martínez-Prieto, C. Urbaneja, P. Palma, J. Campora, K. Philippot, B. Chaudret, *Chem. Comm.* **2015**, *51*, 4647.

S5. MAS NMR data

Before ^{13}CO:

The solid state ^{13}C CP-MAS NMR spectra of Ru@**1** and Ru@**2** (Fig. S9 and S10) show the characteristic peaks of the ligands, confirming the presence of **1** and **2** on the Ru surface.

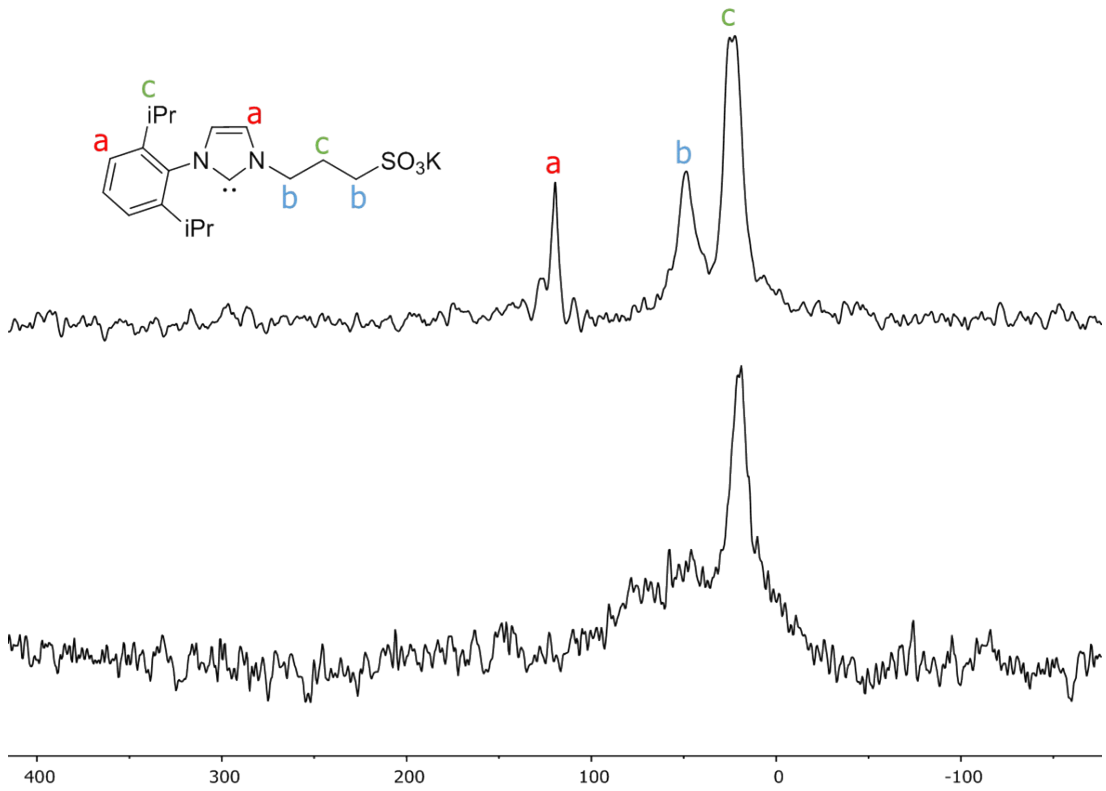

Figure S9. ^{13}C Hahn-echo MAS (bottom) and CP-MAS (top)* NMR spectra of Ru@**1.**

* The signals centred at 119 ppm correspond to the aromatic ring and the imidazolium backbone of the ligand. The peak at 48 ppm belongs to α and γ CH_2 groups of the alkyl chain of the sulfonated N-substituent. The intense peak at 22 ppm correspond to the overlapping of isopropyl groups and the β CH_2 group of **1**. It should be noted that the peak corresponding to the precarbenic carbon of the imidazolium ring was not detected (expected at 145-140 ppm) confirming its deprotonation and formation of the NHC ligands on the Ru surface.

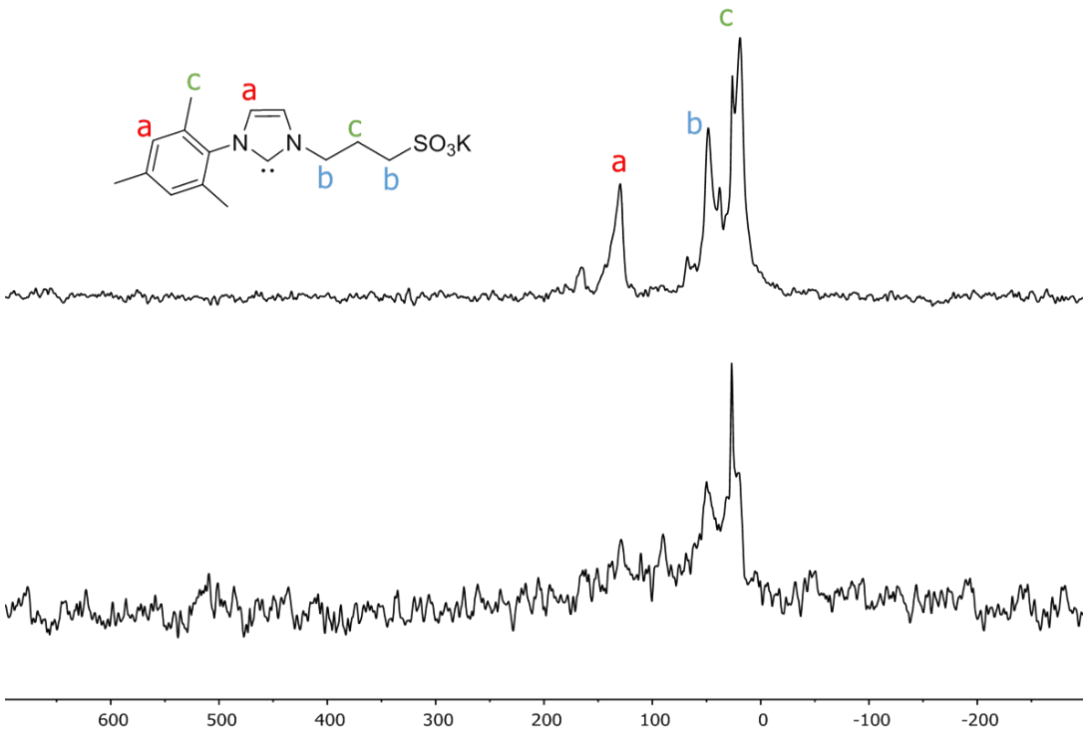

Figure S10. ^{13}C Hahn-echo MAS (bottom) and CP-MAS (top)* NMR spectra of Ru@**2**.

* The signals centred at 135 ppm correspond to the aromatic ring and the imidazolium backbone of **2**. The peak at 48 ppm belongs to α and γ CH_2 groups of the alkyl chain of the sulfonated N-substituent. The peaks at 26 and 19 in Figure S10 are attributed to the *para* and *ortho* methyl groups of **2** with the overlapping of the β CH_2 group of **2** as well. It should be noted that the peak corresponding to the precarbenic carbon of the imidazolium ring was not detected (expected at 145-140 ppm) confirming its deprotonation and formation of the NHC ligands on the Ru surface.

After ^{13}CO:

After pressurizing with 1 bar of ^{13}CO (r.t., 20 h) Ru@**1** and Ru@**2** (Fig. S11), ^{13}C MAS NMR spectra displayed a broad resonance at δ ~ 240 ppm, assigned to ^{13}COb and a sharp peak at δ 198-200 ppm which corresponds to ^{13}COt. In both cases the bridging CO groups are abundant which suggests, by comparison with preceding studies,[4] the presence of readily accessible faces and a relatively low number of coordinated carbene molecules.

[4] a) P. Lara, O. Rivada-Wheelaghan, S. Conejero, R. Poteau, K. Philippot, B. Chaudret, *Angew. Chem. Int Ed.* **2011**, *50*, 12080-12084; *Angew. Chem.* **2011**, *123*, 12286-12290; b) L. M. Martínez-Prieto, A. Ferry, P. Lara, C. Richter, K. Philippot, F. Glorius, B. Chaudret, *Chem. Eur. J*, **2015**, *21*, 17495-17502; c) L. M. Martínez-Prieto, A. Ferry, L. Rakers, C. Richter, P. Lecante, K. Philippot, B. Chaudret, F. Glorius, *Chem. Commun.* **2016**, *52*, 4768-4771

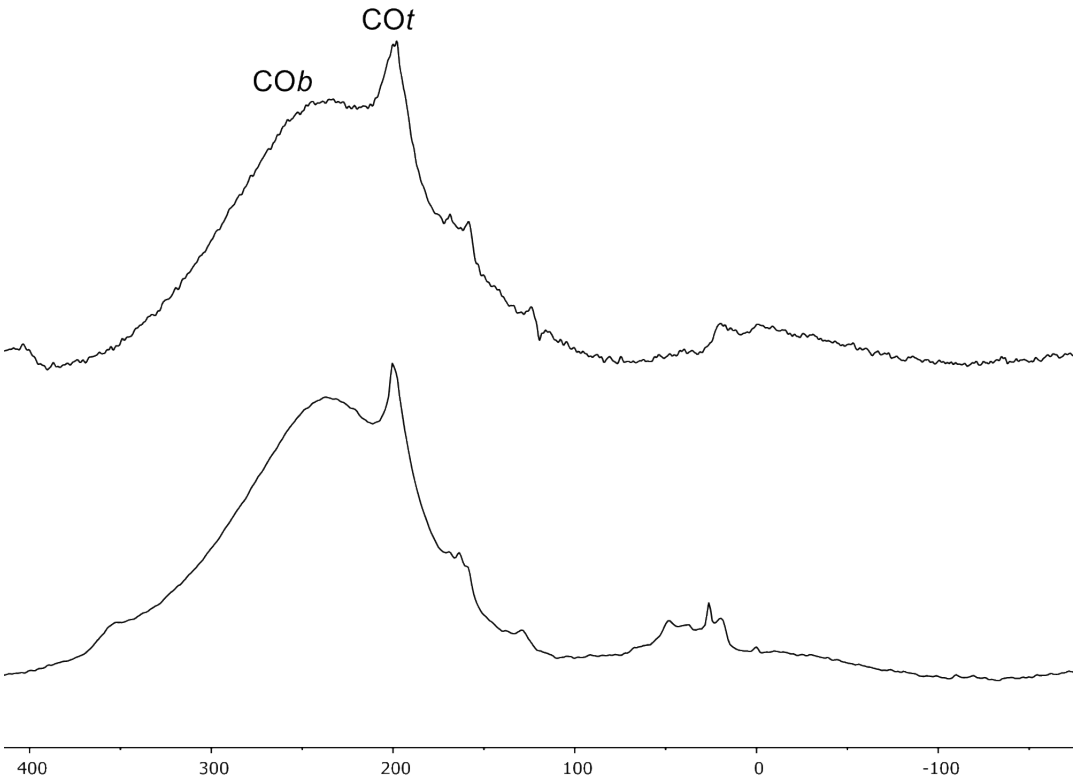

Figure S11. ^{13}C Hahn-echo MAS NMR spectra of Ru@**1** (top) and Ru@**2** (bottom) after exposure to ^{13}CO (1 bar, 20 h, at r.t.).

S6. XPS data

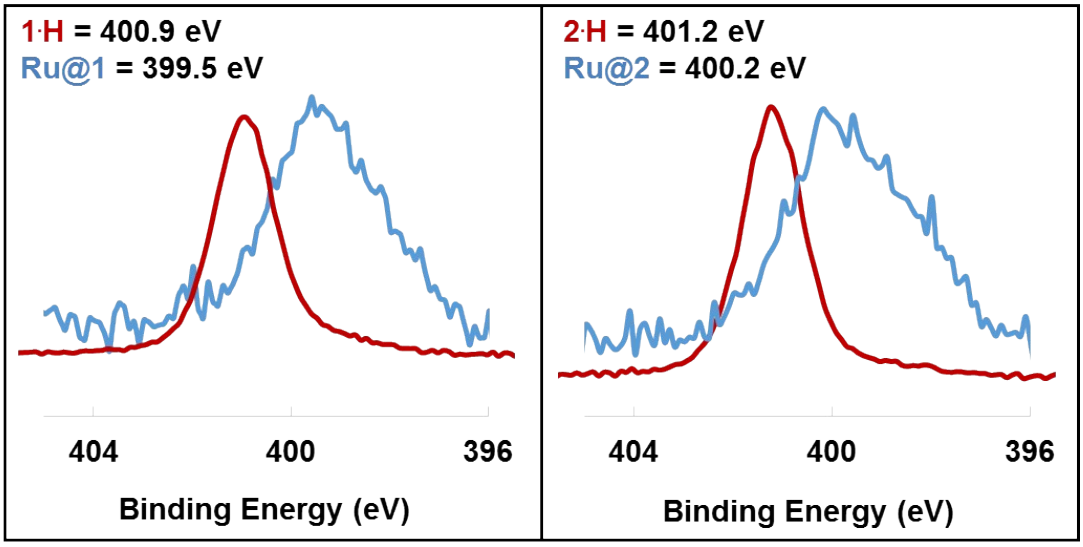

Figure S12. X-ray photoelectron spectra of the N 1s signals of **1**•H (red, left), **2**•H (red, right), Ru@**1** (blue, left) and Ru@**2** (blue, right).*

* Coordination of NHCs on the Ru surface increases the electronic density in the nitrogen atoms and, therefore, lowers the binding energies of the N 1s electrons with respect to the imidazolium cation.

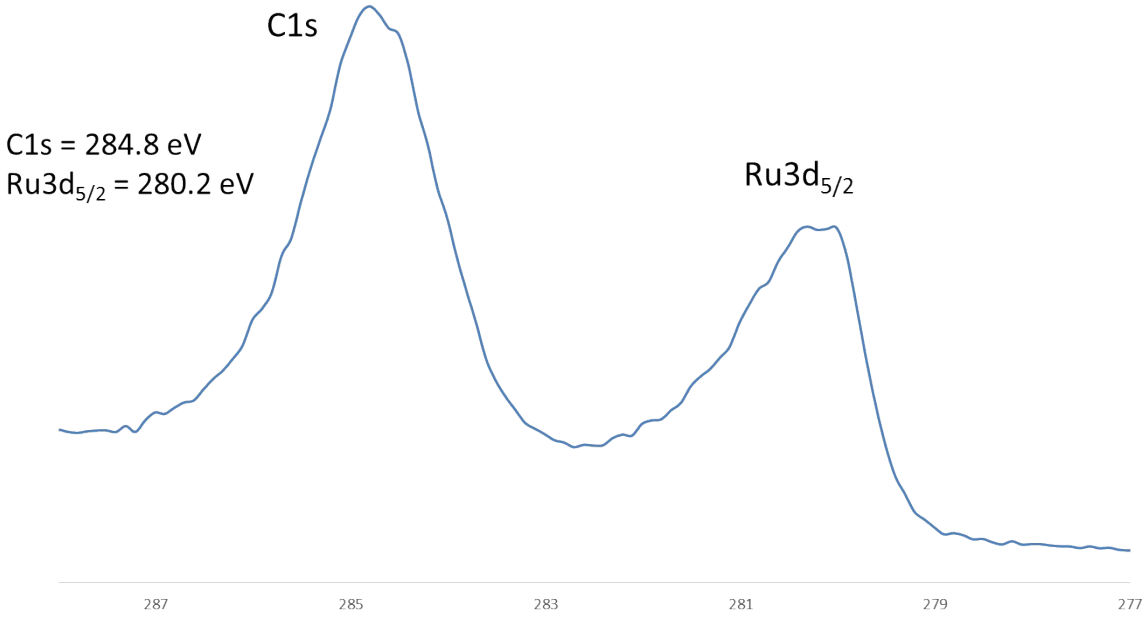

Figure S13. X-ray photoelectron spectrum of the Ru $5d_{5/2}$ signals of Ru@**1**.*

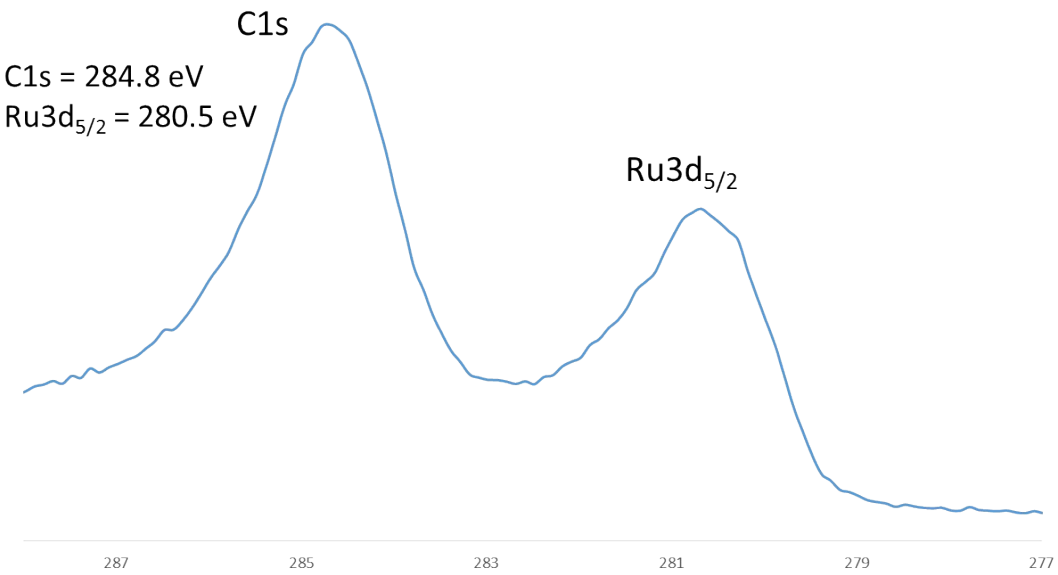

Figure S14. X-ray photoelectron spectruma of the Ru $5d_{5/2}$ signals of Ru@**2**.*

* The main component at BE of 284.8 eV corresponds to the C 1s signal together the Ru $5d_{3/2}$ signals of Ru@**1** and Ru@**2**.

S7. Analytical data

Table S1. Analytical Data of Ru@**1** and Ru@**2**.*

RuNP	Diameter (nm)	Ru Content (%)	Ru/L Ratio	Ru_x/L_y[a]	N_s[b]
Ru@**1**	1.4 (0.2)	58.7	5.36 : 1	119/22	77
Ru@**2**	1.5 (0.3)	60.1	5.16 : 1	138/27	87

[a] The approximate composition is based on the Ru/L ratio and the mean diameter measured by TEM. [b] Number of surface atoms. Approximate values obtained from the graphs of Van Hardeveld and Hartog.[5]

* It is worth noting that the Ru/L ratio is close to three to one which in principle should allow the coordination of all ligands at the surface of the particle. However, given the bulkiness of the ligand, the presence of some ligands in the second coordination sphere cannot be excluded.[6] Nevertheless, as previously observed, for example using CO as a probe molecule, the presence of these bulky ligands leave open coordination sites for reactivity.

[5] . Van Hardeveld, F. Hartog, *Surf. Sci.* **1969**, *15*, 189.

[6] E. A. Baquero, S. Tricard, J. C. Flores, E. de Jesús, B. Chaudret, *Angew. Chem. Int. Ed.* 2014, **53**, 13220.

S7. Catalytic data

General procedure for deuteration reactions

A 100 mL Fisher-Porter reactor was charged with Ru NPs (2 mg, 8 %) and a magnetic stirrer in a glove box under argon. A solution of L-lysine (21.92 mg, 0.15 mmol) in D_2O (2 mL) was added under argon and the reaction mixture was stirred at 55 °C under 2 bar D_2 during 42 hours. After that, the solution was allowed to reach the r.t. The final product was analyzed directly by taking an aliquot from the solution, without the needing of previous purification. The deuterium incorporation was quantified by the decrease of ^1H NMR integral intensities at the specified positions compared to the starting material. Integral intensities were calibrated against hydrogen signals of position β which do not undergo H/D-exchange. This was confirmed by adding 1 equiv. of CH_3CN as internal standard in deuteration of L-lysine at pH = 13.16.

The enantiospecificity was confirmed by HPCL using L-lysine and D-lysine as references. The D_2O solutions after catalysis were directly injected on the HPLC.

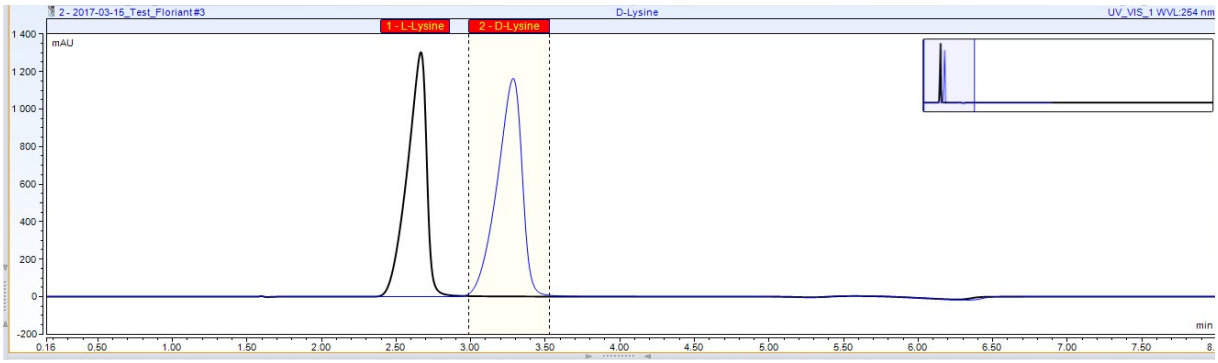

Figure S15. Chromatogram of L-lysine and D-lysine used as references.

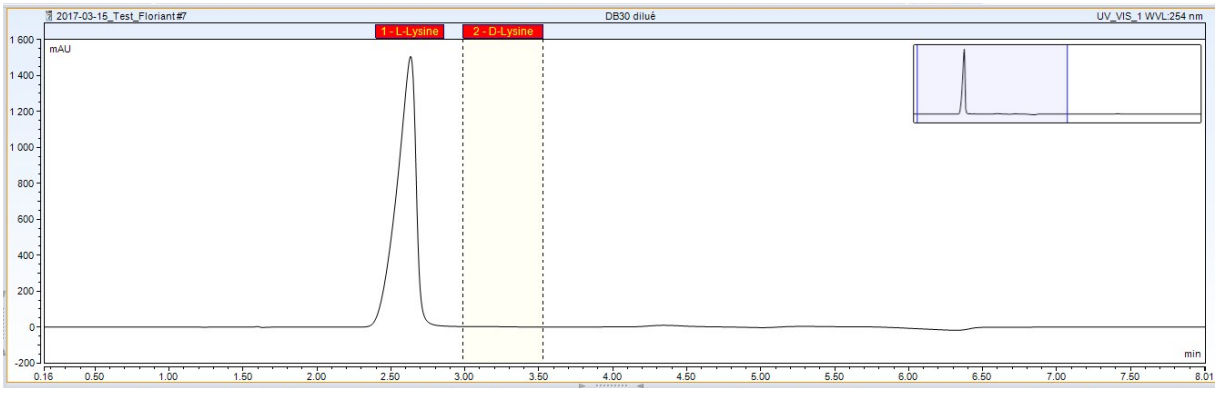

Figure S16. Chromatogram of C–H activation/deuteration of L-lysine using Ru@**1** in D_2O at pH 10.4 (2 bar D_2, 55 °C, 42 h).

Table S1. Enantiospecific C–H activation/deuteration of L-lysine.[a]

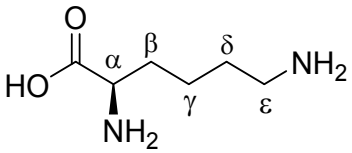

Catalyst	α (%)	β (%)	γ (%)	δ (%)	ε (%)
Ru@PVP	98	0	14.5	0	98.5
Ru@1	99	0	12.5	0	98.5
Ru@2	98	0	4	0	97

[a] Reaction conditions: all experiments were performed in D_2O in the presence of 8% Ru NPs, 2 bar D_2 and 55 °C during 42 h.

L-lysine solutions at different pHs[7].

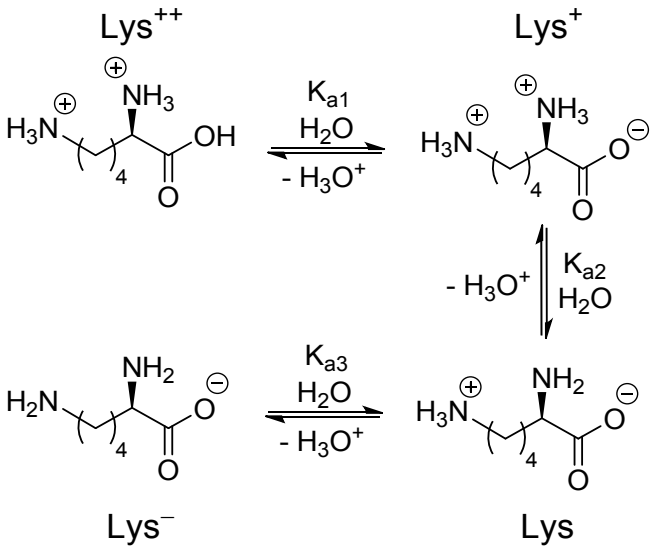

Figure S17. pH dependence equilibriums of the species derived from L-lysine.

Solutions of 0.15 mmol of L-lysine in 2 mL D_2O at different pHs were obtained preparing mixtures of L-lysine•HCl/L-lysine•2HCl (pHs between 1.6 and 3.2), L-lysine/L-lysine•HCl (pHs between 6.9 and 10.4) and L-lysine/NaOD (pHs between 11.0 and 13.8).

[7] The pHs reported where calculated from the corresponding PDs (measures in D_2O with a pH-meter) following the equation pD = pH + 0.45 (A. Krężel, Wo. Bal, *J. Inorg. Biochem*. **2004**, *981*, 161-166).

Table S2. Solutions of L-lysine in D_2O at different pHs.[a]

pH[b]	L-lysine (mg)	L-lysine • HCl (mg)	L-lysine • 2HCl (mg)	NaOD (µL)[c]
1.6	-	-	32.86	-
2.2	-	12.18	18.26	-
3.2	-	24.9	2.99	-
6.9	-	27.4	-	-
8.4	1.98	24.9	-	-
9.1	7.31	18.26	-	-
10.4	21.92	-	-	-
11.0	21.92	-	-	2.5
12.0	21.92	-	-	8
13.2	21.92	-	-	12
13.8	21.92	-	-	100

[a] All solutions are made up of 0.15 mmol of L-lysine in 2 mL D_2O.

[b] pHs between 1.65 and 3.21 were obtained using-buffer solutions of L-lysine•HCl /L-lysine•2HCl. pHs between 6.90 and 10.4 were obtained using buffer solutions of L-lysine/L-lysine•HCl. pHs between 11.01 and 13.81 were obtained adding NaOD into a solutions of L-lysine.

[c] 40 wt. % in D_2O.

S8. Solution NMR data

^{1}H NMR spectrum of Commercial L-lysine:

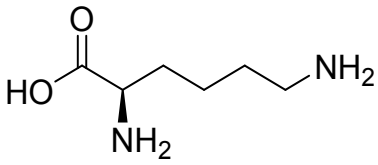

^{1}H NMR (400 MHz, D2O) δ 3.72 (t, *J* = 6.13 Hz, 1H), 2.96 - 3.02 (m, 2H), 1.82 - 1.92 (m, 2H), 1.69 (quin, *J* = 7.64 Hz, 2H), 1.34 - 1.53 (m, 2H).

^{1}H NMR spectra of L-lysine after deuteration with Ru NPs:

1. Ru@PVP:

pH = 10.41

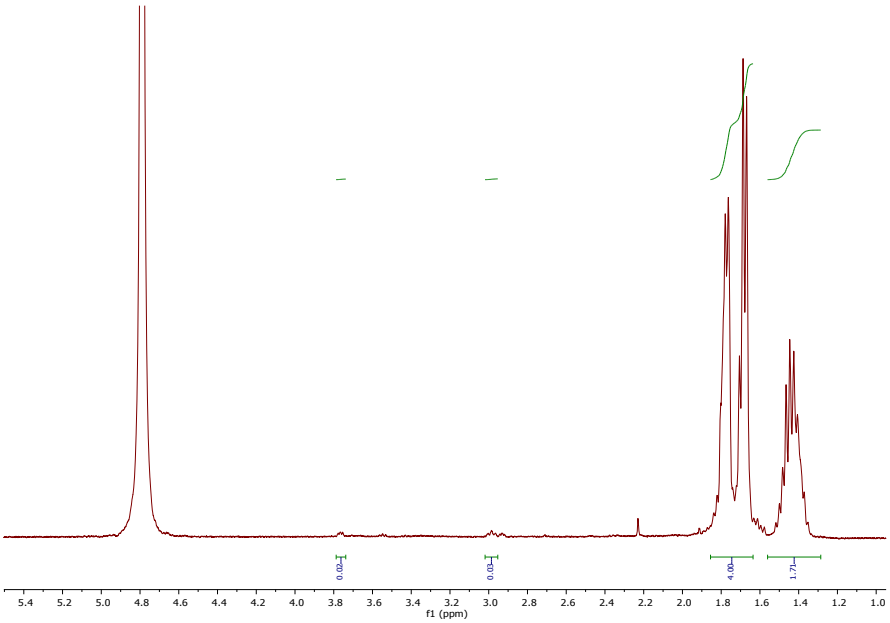

Figure S18. ^{1}H NMR spectrum after deuteration of L-lysine at pH 10.41 using Ru@PVP as catalyst.

2. Ru@2:

pH = 10.41

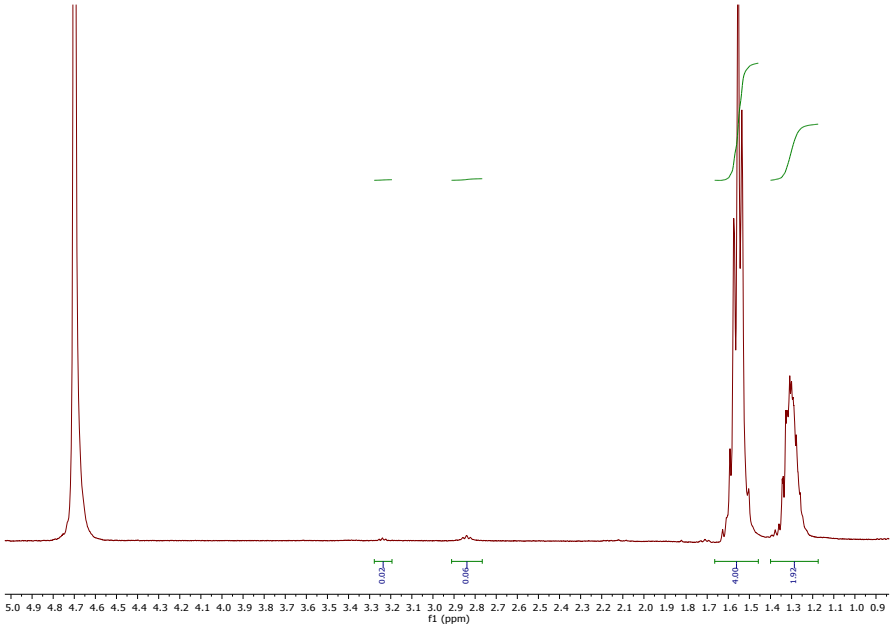

Figure S19. ^{1}H NMR spectrum after deuteration of L-lysine at pH 10.41 using Ru@**2** as catalyst.

2. Ru@1:

pH = 1.65

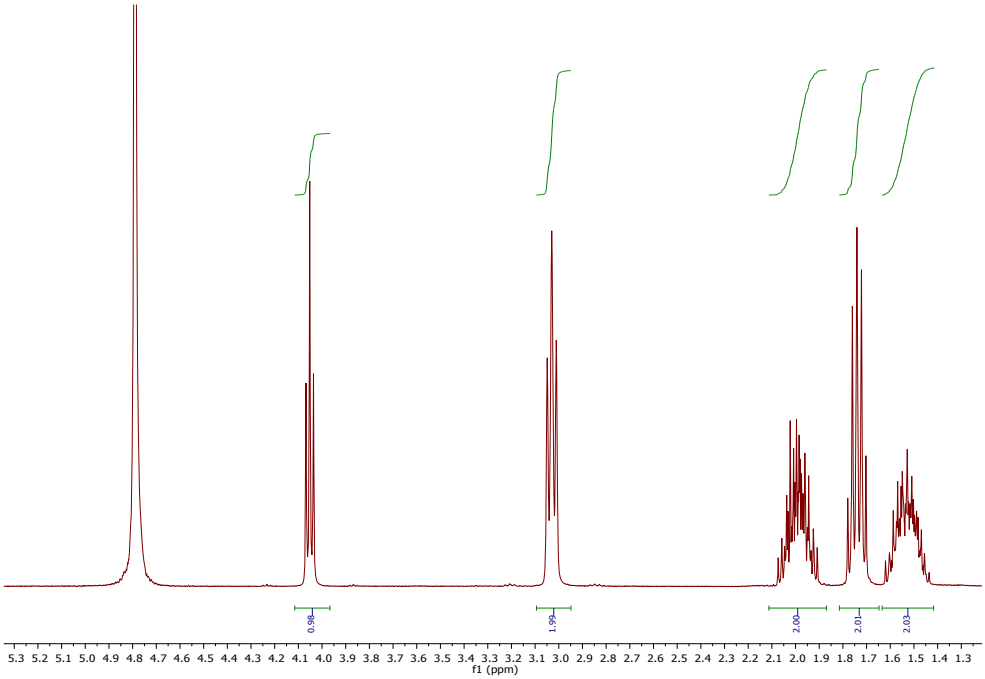

Figure S20. ^{1}H NMR spectrum after deuteration of L-lysine at pH 1.65 using Ru@**1** as catalyst.

pH = 2.19

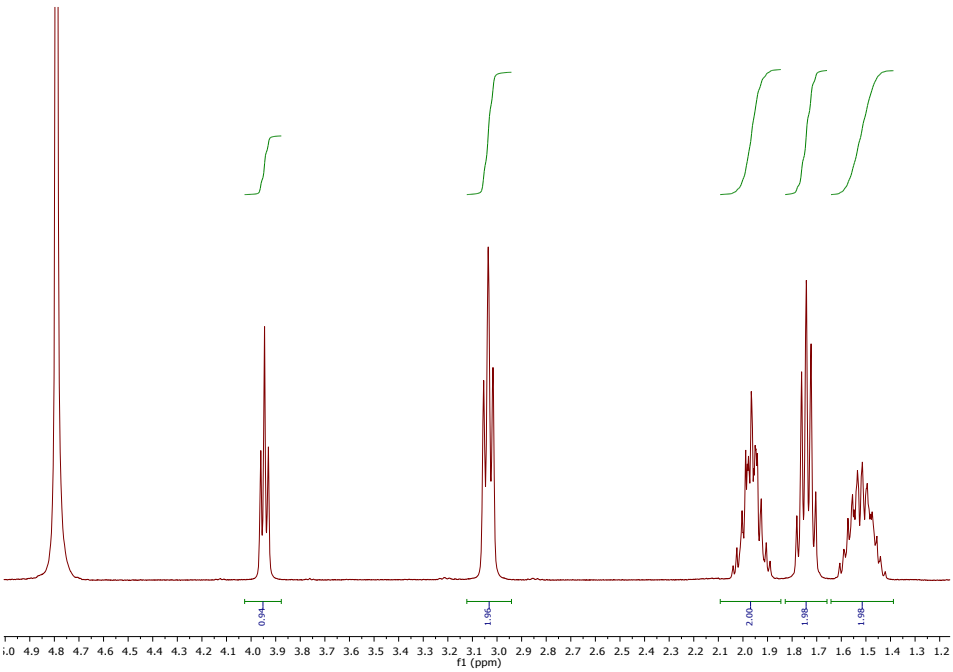

Figure S21. ^{1}H NMR spectrum after deuteration of L-lysine at pH 2.19 using Ru@**1** as catalyst.

pH = 3.21

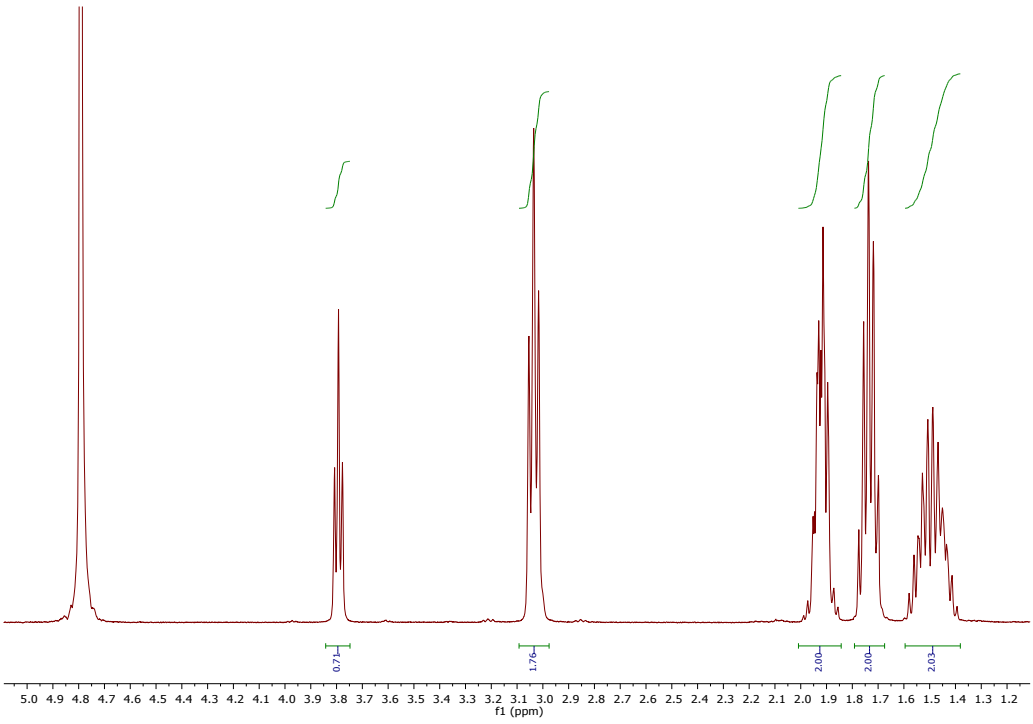

Figure S22. ^{1}H NMR spectrum after deuteration of L-lysine at pH 3.21 using Ru@**1** as catalyst.

pH = 6.90

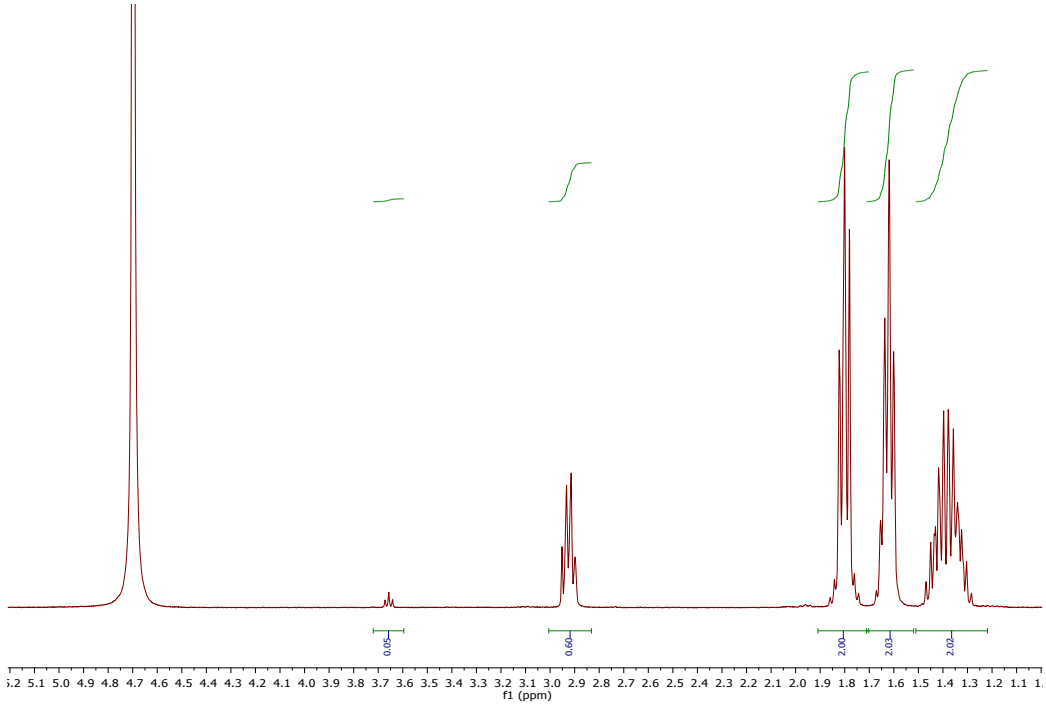

Figure S23. ^{1}H NMR spectrum after deuteration of L-lysine at pH 6.90 using Ru@**1** as catalyst.

pH = 8.45

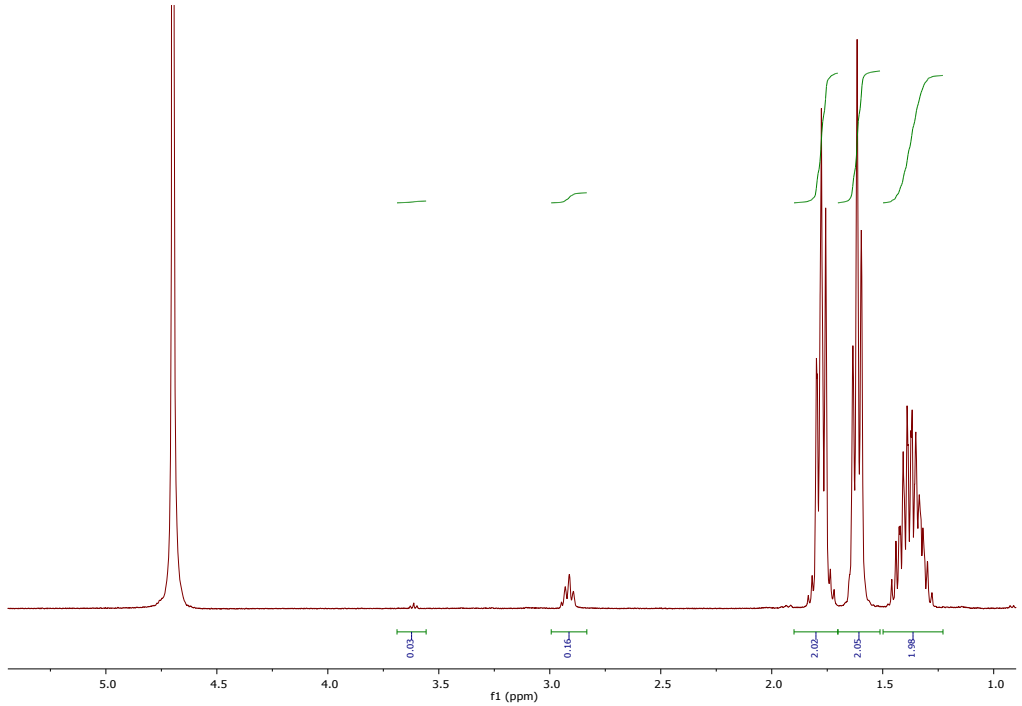

Figure S24. ^{1}H NMR spectrum after deuteration of L-lysine at pH 8.45 using Ru@**1** as catalyst.

pH = 9.10

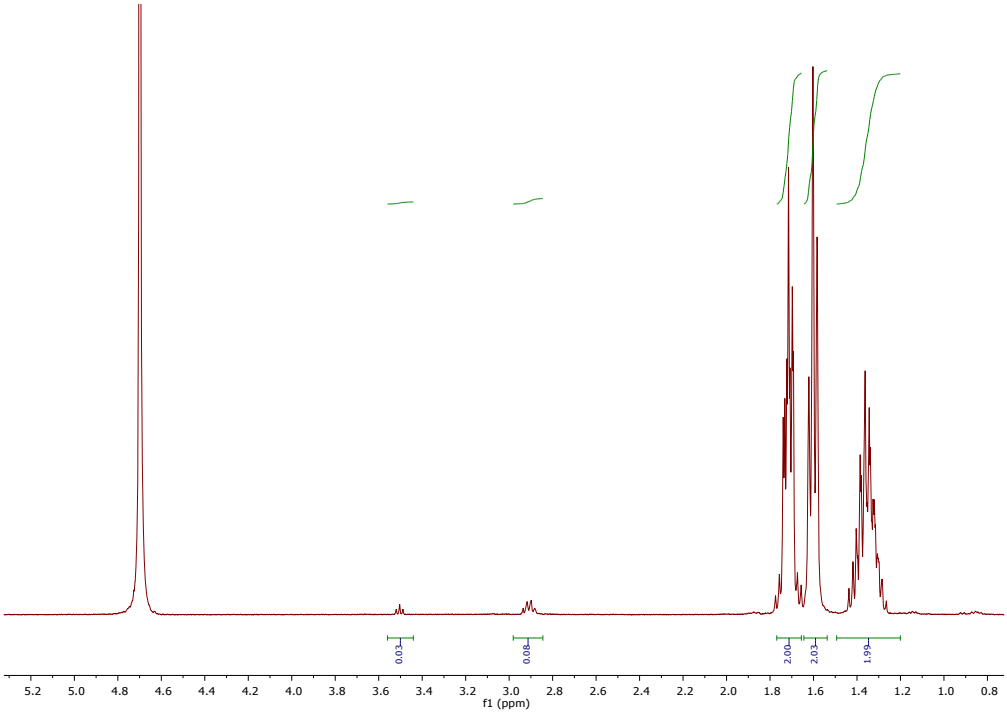

Figure S25. ^{1}H NMR spectrum after deuteration of L-lysine at pH 9.10 using Ru@**1** as catalyst.

pH = 10.41

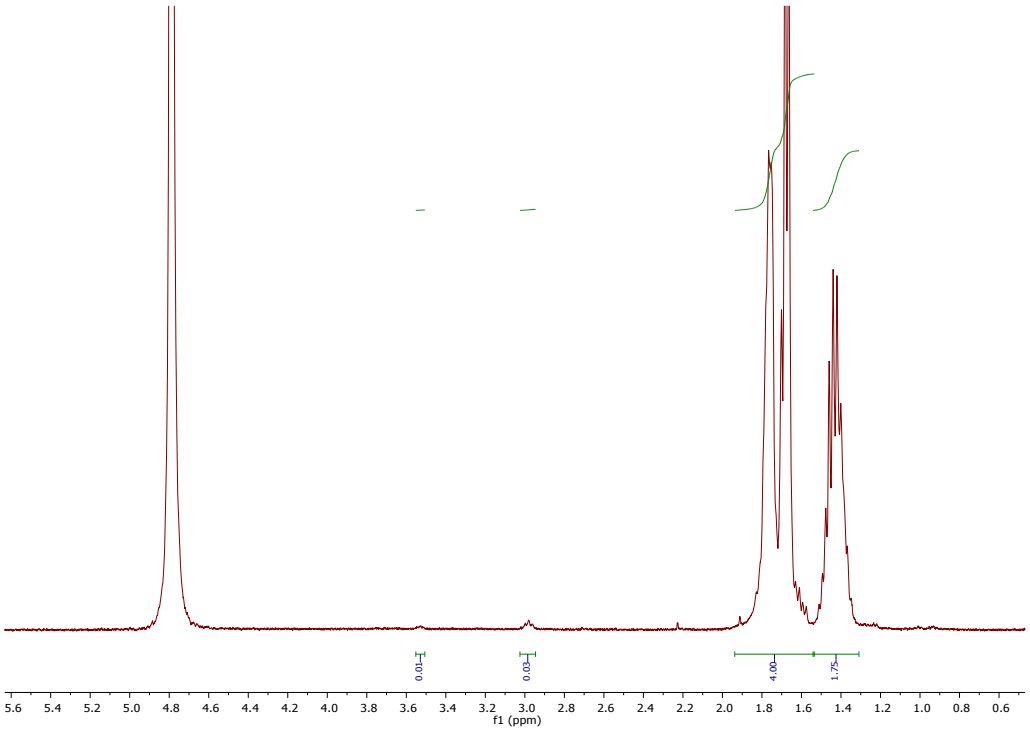

Figure S26. ^{1}H NMR spectrum after deuteration of L-lysine at pH 10.41 using Ru@**1** as catalyst.

pH = 11.01

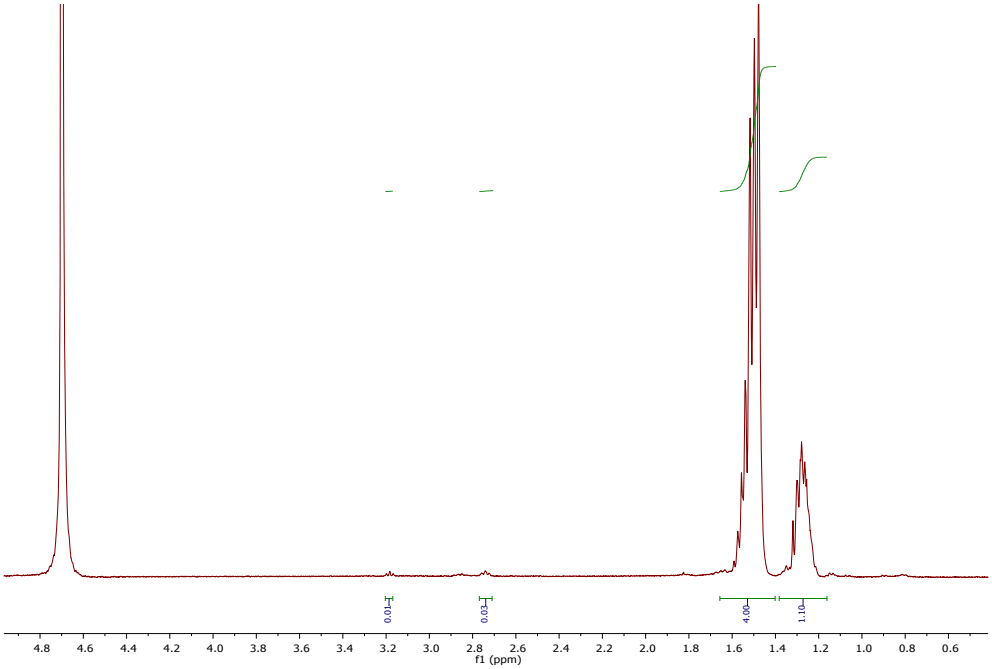

Figure S27. ^{1}H NMR spectrum after deuteration of L-lysine at pH 11.01 using Ru@**1** as catalyst.

pH = 12.02

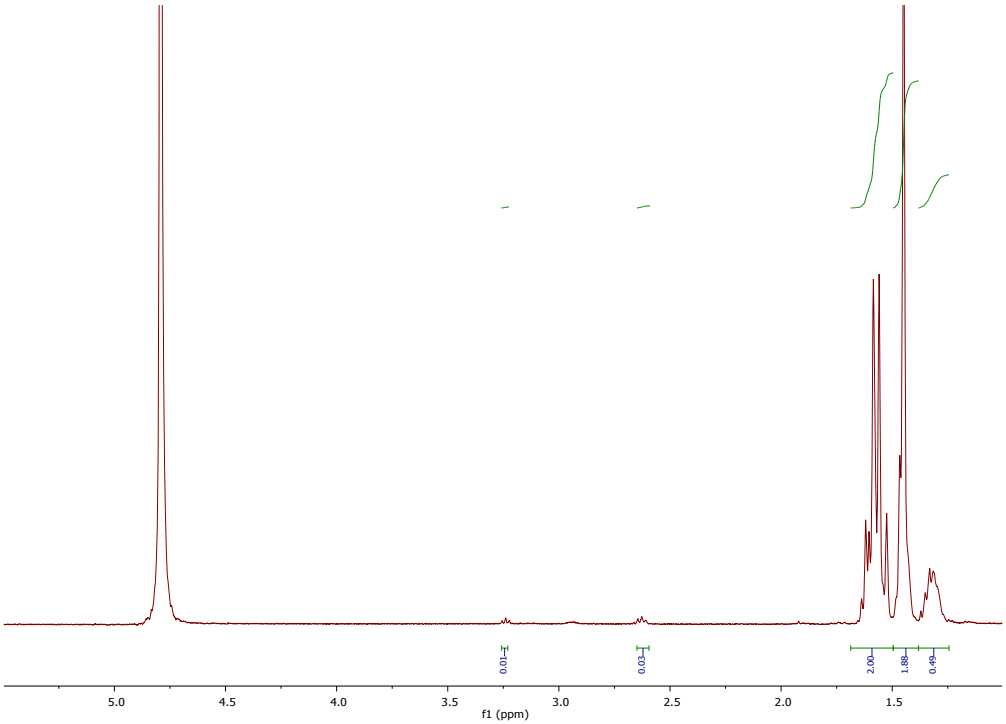

Figure S28. ^{1}H NMR spectrum after deuteration of L-lysine at pH 12.02 using Ru@**1** as catalyst.

pH = 13.16

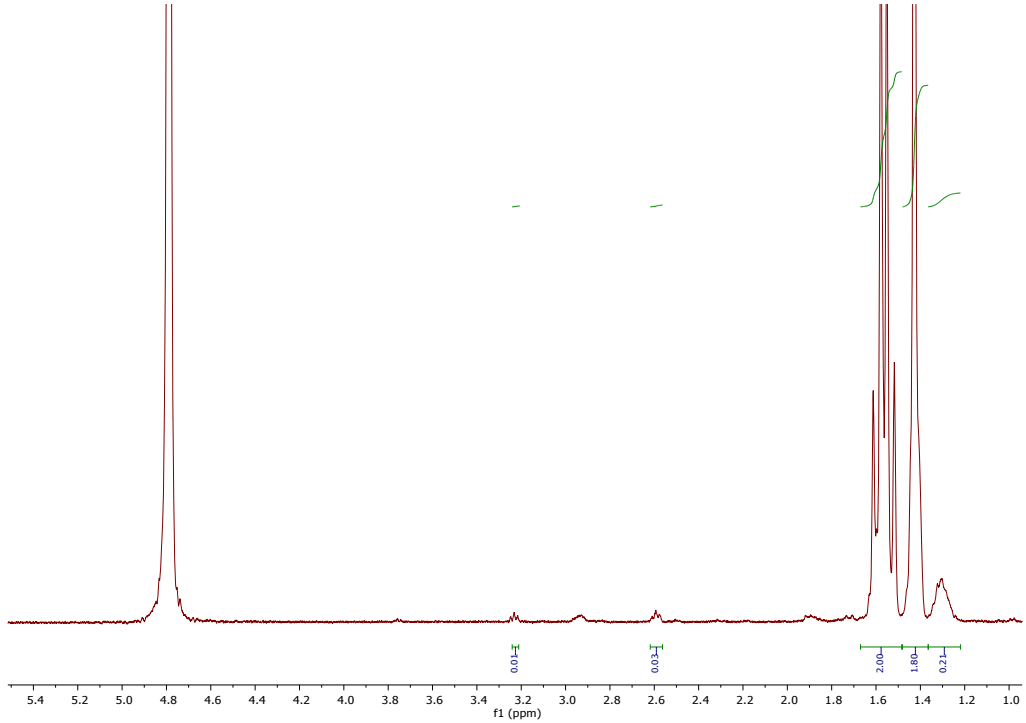

Figure S29. ^{1}H NMR spectrum after deuteration of L-lysine at pH 13.16 using Ru@**1** as catalyst.

pH = 13.81

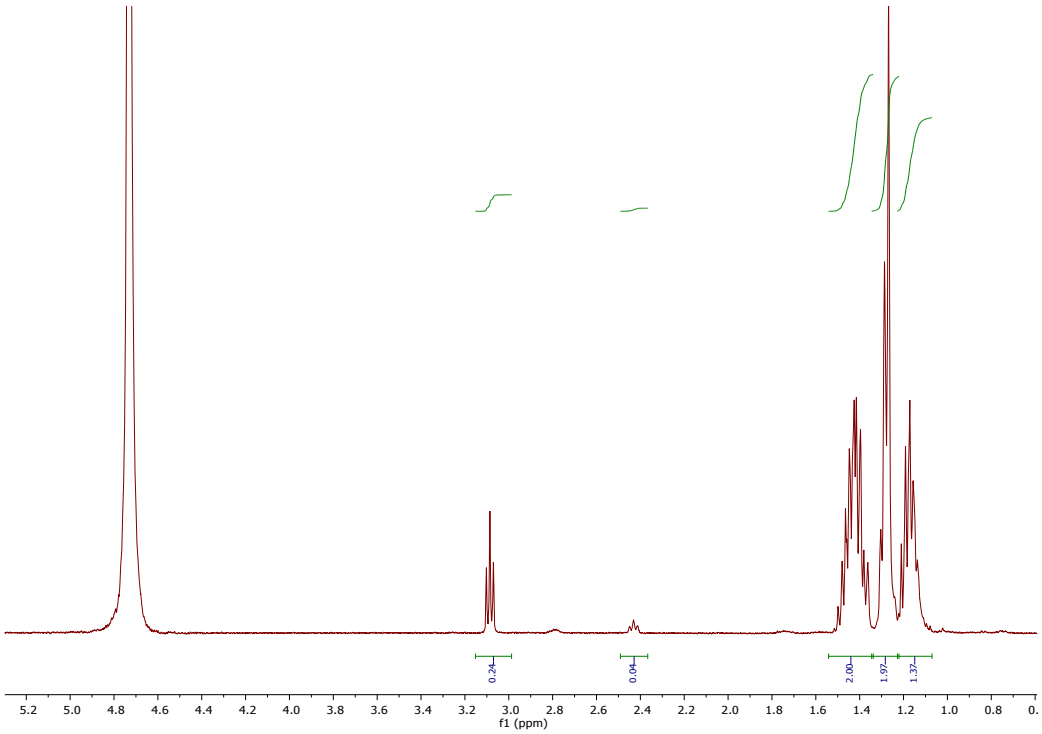

Figure S30. ^{1}H NMR spectrum after deuteration of L-lysine at pH 13.81 using Ru@**1** as catalyst.

S9. NMR Interaction studies

^{1}H, ^{13}C HSQC spectra of different amounts of L-lysine with 1 mg/mL of NPs were recorded at different pH values, as described above. Spectra were recorded at natural abundance on an 800MHz Bruker NMR spectrometer, equipped with a QCP cryogenic probehead. We used a sensitivity enhanced HSQC sequence[8] with 2048 × 256 points for the ^{1}H respectively ^{13}C dimension, corresponding to a spectral window of 13.9486 × 40.0000 ppm. We recorded 2 scans per increment, arriving at a total measuring time of 10 minutes per spectrum. Samples with NPs were intensely vortexed for two minutes just before the measurement, to avoid any possible sedimentation.

For each pH value and L-lysine concentration, we recorded a spectrum in the absence and presence of the NPs. For the samples at low (~6.9) and high (~13.4) pH values, where the concentration did influence the pH value, the resulting pH dependence of the resonance shift was compensated for by referencing all spectra in the absence of NPs to a common chemical shift for a given peak, and applying the subsequent spectral referencing to the corresponding spectra in the presence of NPs. For the L-lysine samples at pH 10.4, the pH was stable irrespective of the concentration. We show in Figures S31 to S33 the corresponding chemical shift perturbations of the different L-lysine resonances at pH 13.2, pH 10.4 and pH 6.9.

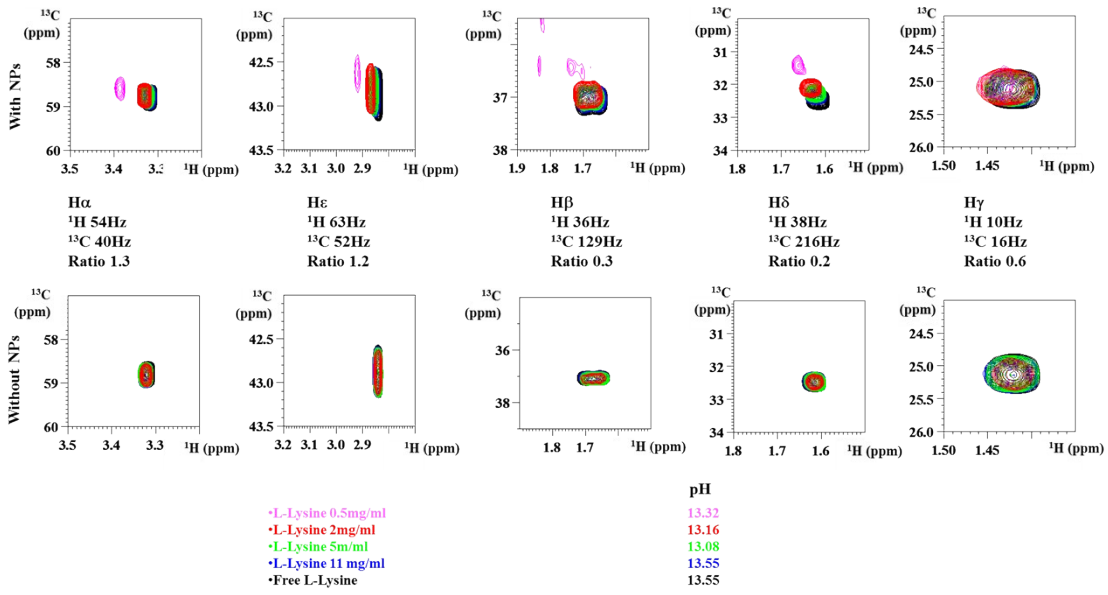

Figure S31. ^{1}H, ^{13}C HSQC spectra of D_2O solutions of free L-lysine (black), 1 mg/mL of Ru@**1** with 11 (blue), 5 (green), 2 (red) and 0.5 (magenta) mg of L-lysine at pH ~ 13. The lower row shows the spectra of the free L-lysine at different concentrations, whereby the pH dependence was taken into account by referencing the individual peaks to their value in the spectrum of free L-lysine at 22 mg/mL. This spectral reference was then used to remove the pH dependence of the spectra in the presence of NPs (upper row).

[8] A.G. Palmer III, J. Cavanagh, P.E. Wright, M. Rance, *J. Magn. Reson.* **1991**, *93*, 151-170.

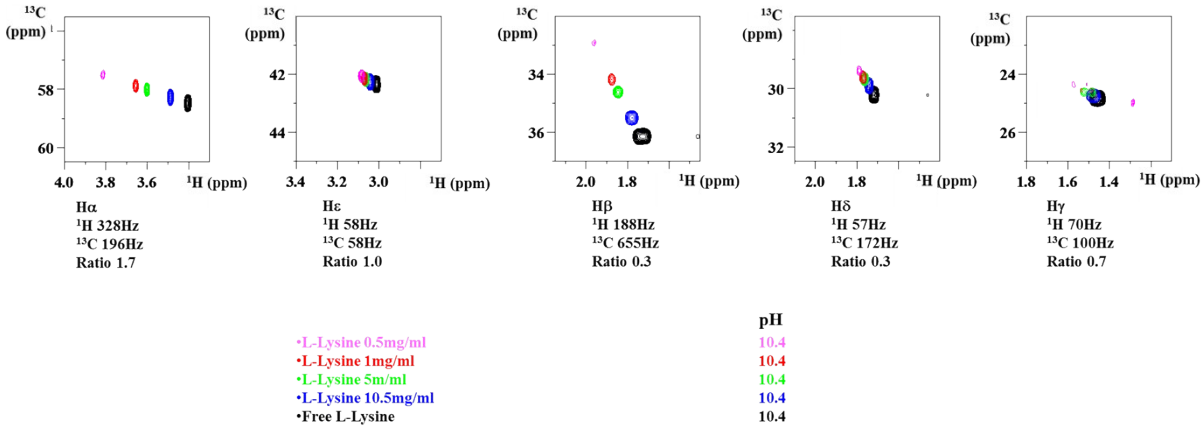

Figure S32. ^{1}H, ^{13}C HSQC spectra of D_2O solutions of free L-lysine (black), 1 mg/mL of Ru@**1** with 11 (blue), 5 (green), 2 (red) and 0.5 (magenta) mg of L-lysine at pH = 10.4.

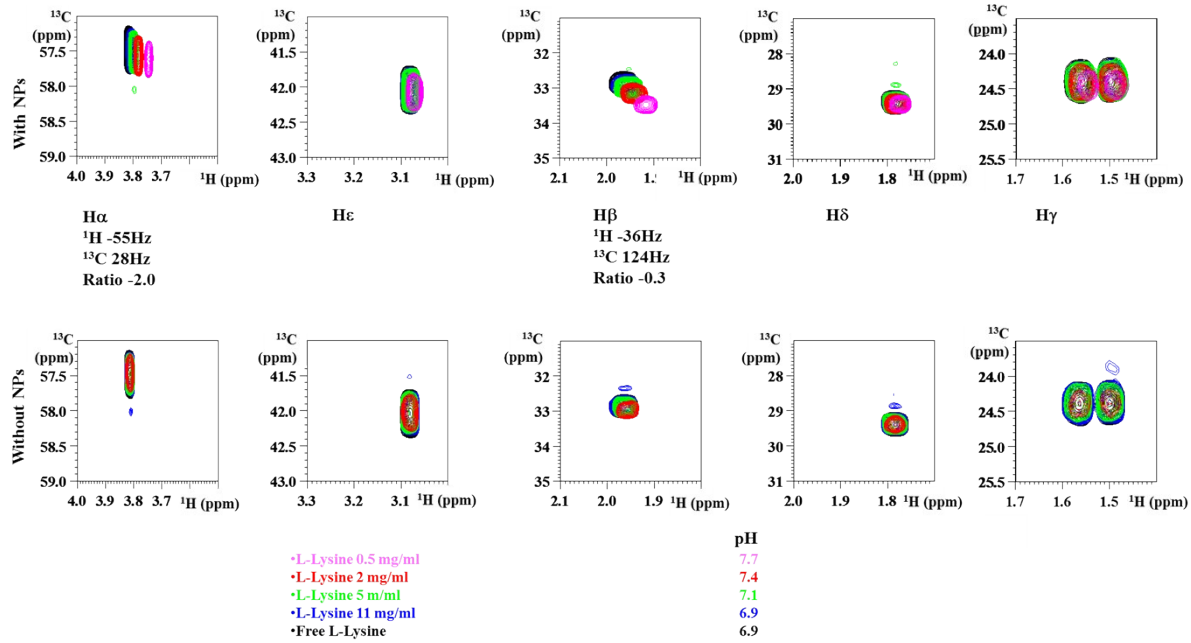

Figure S33. ^{1}H, ^{13}C HSQC spectra of D_2O solutions of free L-lysine (black), 1 mg/mL of Ru@**1** with 11 (blue), 5 (green), 2 (red) and 0.5 (magenta) mg of L-lysine at pH ~ 7. The lower row shows the spectra of the free L-lysine at different concentrations, whereby the pH dependence was taken into account by referencing the individual peaks to their value in the spectrum of free L-lysine at 22 mg/mL. This spectral reference was then used to remove the pH dependence of the spectra in the presence of NPs (upper row).

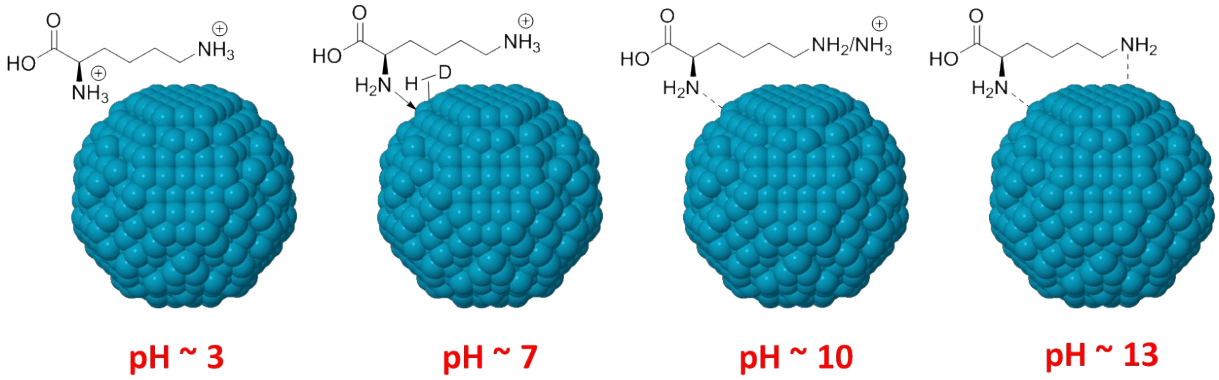

Figure S34. Interaction of L-lysine with Ru NP surface as a function of pH.